

## Experimental study on dynamic shear modulus and damping ratio of CAS-1 lunar regolith simulant

F. Yu\*, Sh.X. Chen, Y. Zhang, J. Li, Zh.J. Dai

State Key Laboratory of Geomechanics and Geotechnical Engineering, Institute of Rock and Soil Mechanics, Chinese Academy of Sciences, Wuhan, Hubei, 430071, China

Received September 1, 2017; Accepted December 19 2017

In the paper an experimental study of the dynamic parameters of CAS-1 lunar regolith simulant is carried out, and the law by which different void ratios and confining pressures influence the dynamic shear modulus  $G$  and the damping ratio  $\lambda$  is analyzed. The test results show that, in the case of real lunar surface under very low stress levels and large void ratio, the dynamic shear modulus  $G$  is smaller, and the damping ratio  $\lambda$  is larger; the dynamic shear modulus diminishes quickly and the damping ratio increases sharply along with the increase of dynamic shear strain  $\gamma$ . Using the Hardin-Drnevich Model, the paper comes to the average fitted curve of the normalized dynamic shear modulus  $G/G_{\max}$  and the normalized damping ratio  $\lambda/\lambda_{\max}$  changing with  $\gamma$  on the conditions of different void ratios and confining pressures. The correlative equation between the maximum dynamic shear modulus  $G_{\max}$ , the maximum damping ratio  $\lambda_{\max}$ , the dynamic parameters such as the reference shear strain  $\gamma_r$  and the stress levels  $\sigma$  are discussed. Based on this, the range intervals of  $G_{\max}$ ,  $\lambda_{\max}$  and  $\gamma_r$  within the coring and sampling depth (0~3m) of lunar regolith, as well as the recommended values of  $G/G_{\max}$  and  $\lambda$  corresponding to various shear strain are presented.

**Key words:** CAS-1 lunar regolith simulant, Dynamic shear modulus, Damping ratio, Dynamic shear modulus ratio

### INTRODUCTION

As the key to the Lunar Exploration Phase 3 Program, “Lunar soil sampling” aims to obtain lunar regolith samples of stratification quality. However, in the process of sampling, a key problem may be the dynamic response resulting from interactions between the coring device and lunar regolith under particular environmental conditions of the lunar surface. Lunar regolith samples are so precious that even the United States, which already have 381 kg of lunar regolith samples, are very strict and prudent in using them. It is for this reason that the paper carefully chooses a “lunar regolith simulant” [1] with similar mechanical properties to real lunar soil in order to carry out this basic mechanical experimental study.

Scholars at home and abroad [1-12] have conducted relevant research on the physical and mechanical properties of different lunar regolith simulants. Zheng *et al.* [2] mainly studied the microwave dielectric property of CAS-1 lunar regolith simulant; Li *et al.* [7-8] discussed the basic physical and mechanical properties of the lunar regolith simulant made of volcanic ash in Jilin Province of China; Jiang *et al.* [9,10] explored the effects of grain grading and moisture content on the mechanical property of TJ-1 lunar regolith simulant, and carried out a relevant experimental study on the bearing characteristics of TJ-1 lunar regolith simulant. Haydar *et al.* [11] conducted experiments on the tensile property of JSC-1 lunar regolith

simulant and discussed how the weight and thickness of the lunar regolith simulant influence the tensile strength. Robert *et al.* [12] observed and analyzed the micro structure of lunar regolith simulant and performed studies on the improvement of mechanical properties of lunar regolith simulant.

All studies mentioned above are oriented to statics of lunar regolith simulant and focus mainly on its basic physical and mechanical properties. In contrast, few studies are about the dynamic properties or are relevant to lunar regolith coring. Therefore, the present paper will carry out a relevant basic dynamic experimental study by using the CAS-1 lunar regolith simulant (national standard sample) which is jointly developed by the Institute of Geochemistry and the National Astronomical Observatories, Chinese Academy of Sciences in replace of real lunar soil. The dynamic shear modulus and damping ratio are two primary parameters of the dynamic properties of soil and indispensable dynamic parameters for studying the dynamic properties of the soil layer. Consequently, carrying out a dynamic property analysis of dynamic shear modulus and damping ratio of lunar regolith simulant serves as a significant basis for studying the mutual effects between lunar regolith and sampling device.

The lunar surface features a special environment of waterless dryness and weightlessness (1/6  $g$ ), and the compactness looseness of lunar soil is differently distributed in breadth and depth. Based on the facts, the paper will use GDS resonant column apparatus to carry out dynamic property tests of lunar regolith simulant with different void

\*To whom all correspondence should be sent:  
E-mail: yufei8720@163.com

ratios in a series of different low confining pressures and regular confining pressure of the ground. It tries to find out the varying pattern of dynamic shear modulus and damping ratio of lunar regolith simulant subjected to dynamic load, and then uses theoretical analysis to work out the average varying curves of  $G/G_{\max} - \gamma$  and  $\lambda/\lambda_{\max} - \gamma$  and relevant dynamic parameter values. Furthermore, the paper quantitatively analyzes the law by which the confining pressure affects different test results, and finally, it presents the reference values of dynamic modulus and damping ratio within the strain range, resulting from change of confining pressure of lunar regolith simulant with different void ratios.

## TEST SCHEME

### *Experimental equipment*

The experimental apparatus to be used in the study is the Stokoe-type resonant column apparatus (RCA) produced by the British GDS Instruments Company. Its principle is elaborated in Bai's studies [13,14].

### *Experimental material*

The experimental material is CAS-1 lunar regolith simulant (national standard sample) [2] successfully developed by the Institute of Geochemistry and the National Astronomical Observatories, Chinese Academy of Sciences. The particles of CAS-1 lunar regolith simulant are typical grinded particles in angular shape [2], similar to the particle morphology of the world famous JSC-1 lunar regolith simulant [3] which also has conspicuous grinding vestiges.

Through the specific gravity bottle test, the relative density  $G_s$  is worked out to be 2.66, which falls into the category of relative density (2.3~3.2) [15] of real soil particles. The gradation of particles of CAS-1 lunar regolith simulant is between the upper and lower limits of parts of real lunar soil.

### *Test method*

In advance of the experiment, the test samples of lunar regolith simulant were oven-dried and cooled to room temperature. By controlling the void ratio of lunar regolith simulant, the void ratio  $e$  of lunar regolith simulant in two different degrees of looseness was set to be 1.0 and 0.8, respectively. According to the specific gravity, their corresponding initial dry density  $\rho_d$  was 1.33 g/cm<sup>3</sup> and 1.48 g/cm<sup>3</sup>.

During the test, the confining pressure was set at two stress levels: low confining pressure (25, 50, 75, 100 kPa) and regular confining pressure (150, 200, 250, 300 kPa). The excitation voltage applies to CAS-1 lunar regolith simulant. Prior to the

confining pressure test at each level, stabilize for 30 minutes and do not conduct the tests until the LVDT sensor placed on the rotary plate detects the stability of axial settlement amount of the test samples.

## TEST RESULTS

Under different stable confining pressures, the relation curves between dynamic shear modulus  $G$  and shear strain  $\gamma$  of lunar regolith simulant of different compactness are presented in Figure 1. As can be seen,  $G$  gradually diminishes with the increase of  $\gamma$ . When the shear strain is smaller,  $G$  diminishes more slowly, and when shear strain increases to a certain extent, the dynamic shear modulus begins to diminish quickly. The change of dynamic shear modulus along with shear strain reflects the non-linear and hysteretic law of the dynamic stress-strain relationship of the soil [16].

By comparing the test results under different confining pressures, it can be seen that  $G$  decreases with the decrease of confining pressure. On the condition of the same excitation voltage, the shear strain is larger and the trend of dynamic shear modulus diminishing with the increase of shear strain is even more conspicuous.

By comparing the test curves of different void ratios it can be seen that the larger the void ratio, the smaller is the dynamic shear modulus  $G$ . On the condition of the same excitation voltage, the shear strain is larger, and the dynamic shear modulus-shear strain curve is steeper. This means that  $G$  diminishes rapidly with the increase of shear strain and there is no obvious flatness.

Figure 2 shows the relation curves between damping ratio  $\lambda$  and shear strain  $\gamma$  of lunar regolith simulant with different compactness under the condition of different confining pressures. It can be seen from the diagram that the damping ratio increases with the increase of shear strain, and when shear strain increases to a certain extent, the damping ratio increases sharply. By comparing Figure 1 with Figure 2, it is seen that the stage during which the dynamic shear modulus diminishes quickly is exactly the stage where the damping ratio increases rapidly. By comparing the test results of different confining pressures, it can be seen that the smaller the confining pressure, the larger is the damping ratio. On the condition of a small shear strain, the effect of confining pressure on damping ratio is small, but with the increase of shear strain, the effect of confining pressure on damping ratio is dramatically enlarged.

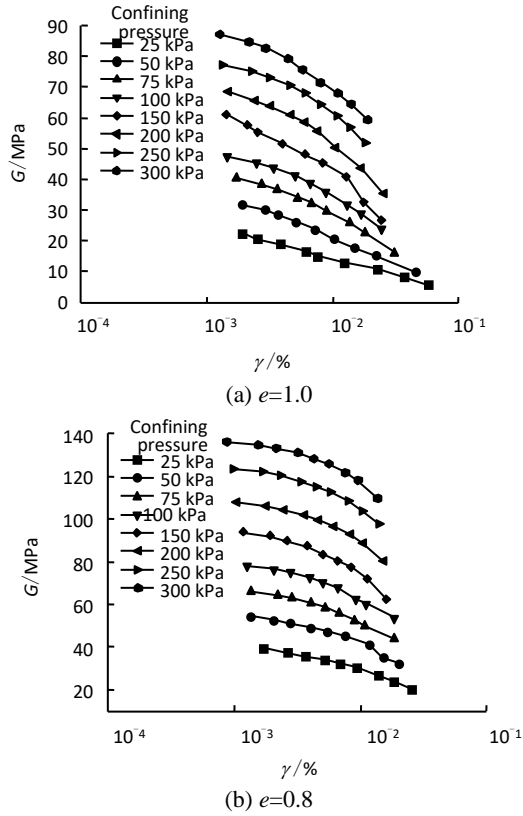


**Fig. 1.** Relationships between dynamic modulus  $G$  and shear strain  $\gamma$  of lunar regolith simulant.

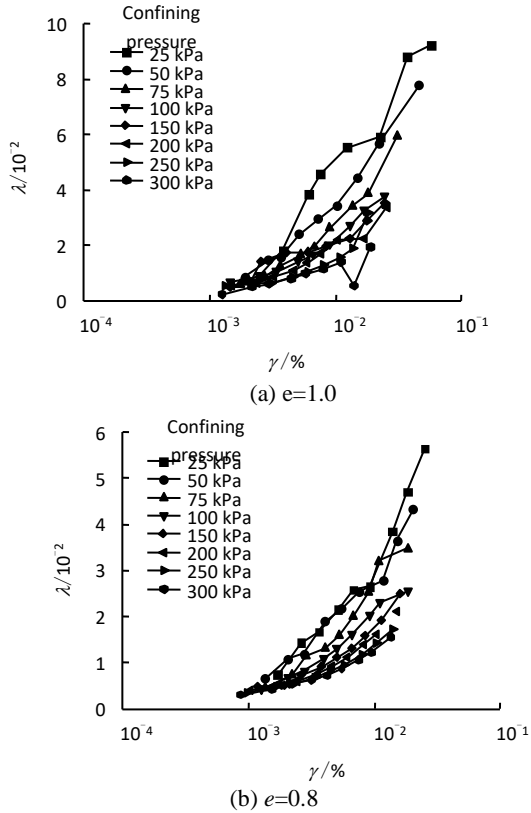


**Fig. 2.** Relationships between damping ratio  $\lambda$  and shear strain  $\gamma$  of lunar regolith simulant.

By comparing the test results of different void ratios, it can be seen that the larger the void ratio, the larger is the damping ratio, and the steeper is the

damping ratio-shear strain curve.

The above test results show that: the stress levels and compactness exert a significant influence on the dynamic shear modulus  $G$  and the damping ratio  $\lambda$  of lunar regolith simulant; under circumstances of real lunar surface, when the stress level is very low and the void ratio is large, the touch points between lunar soil particles are few, resulting in slow transmission of tress wave in lunar soil and are represented by a smaller  $G$  and a larger  $\lambda$ ; and with the increase of shear strain, the dynamic shear modulus diminishes rapidly whereas the damping ratio sharply increases. Such a property has significant effects on the lunar soil coring rate and completeness of the sample.

## ANALYSIS OF TEST RESULTS

### Analysis of test data

As is shown by the test results, the test curves are of good regularity. By using the famous Hardin-Drnevich [17] Hyperbolic Model, the dynamic stress-strain relationships can be described as follows:

$$G = \frac{\tau}{\gamma} = \frac{G_{\max}}{1 + \gamma/\gamma_r} \quad (1)$$

$$\lambda = \lambda_{\max} (1 - G/G_{\max}) \quad (2)$$

$$\gamma_r = \frac{\tau_{\max}}{G_{\max}} \quad (3)$$

Therefore,

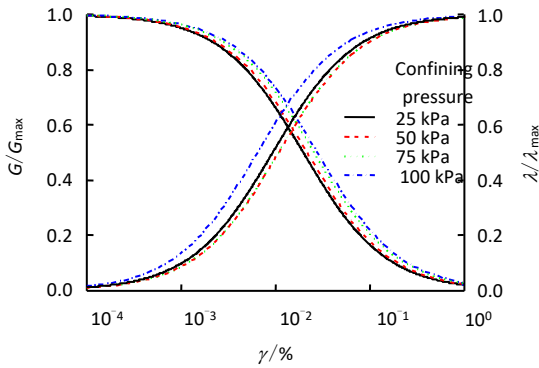
$$G/G_{\max} = \frac{1}{1 + \gamma/\gamma_r} \quad (4)$$

$$\lambda/\lambda_{\max} = \left( \frac{\gamma/\gamma_r}{1 + \gamma/\gamma_r} \right) \quad (5)$$

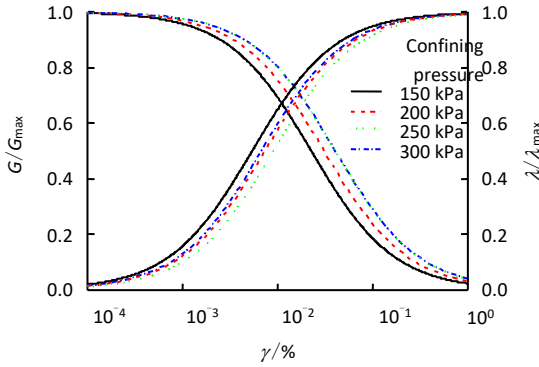
In the equation,  $\tau$  and  $\gamma_r$  are dynamic shear stress and reference shear strain respectively;  $G_{\max}$ ,  $\lambda_{\max}$  and  $\tau_{\max}$  are the maximum dynamic shear modulus, the maximum damping ratio and the maximum dynamic shear stress, respectively.  $G_{\max}$  and  $\lambda_{\max}$  can be measured by the resonant column test, with the results shown in Table 2.

The relationships between dynamic shear modulus, damping ratio and shear strain were experimentally measured. Conduct regression analysis of them by using (1) ~ (5) and the least square method, and make equalization [18,19] of the results from different test regressions. The results are presented in Figure 4.

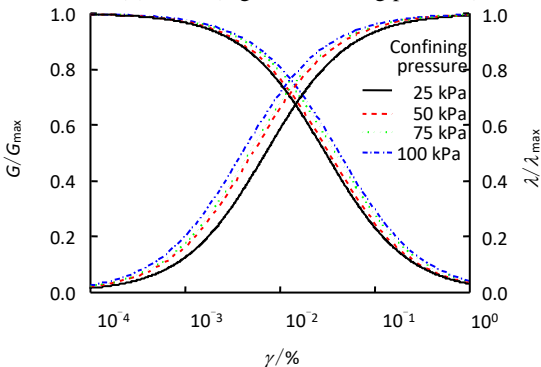
It follows from Figure 4 that the Hardin-Drnevich Hyperbolic Model is suitable for describing the dynamic constitutive relationship of lunar regolith simulant.



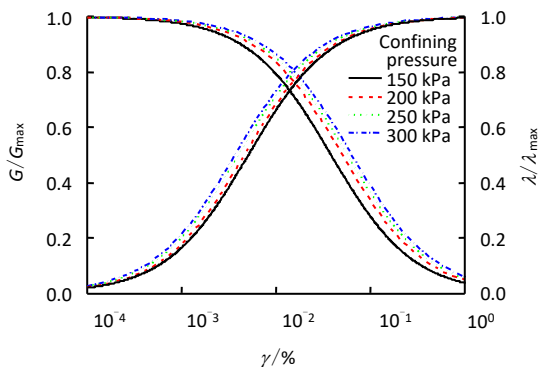
(a)  $e=1.0$  (low confining pressure)



(b)  $e=1.0$  (regular confining pressure)



(c)  $e=0.8$  (low confining pressure)



(d)  $e=0.8$  (regular confining pressure)

**Fig. 4.**  $G/G_{max}$ - $\gamma$  and  $\lambda/\lambda_{max}$ - $\gamma$  experimental curves of different pore ratios of lunar regolith simulant under different confining pressures.

*Varying pattern of  $G_{max}$*

Figure 5 shows that  $G_{max}$  is in a good linear relationship with the confining pressure  $\sigma$  (25 ~

300kPa) and increases with the increase of confining pressure  $\sigma$ . The expression is as follows:

$$G_{max} = A_1 + B_1\sigma \quad (6)$$

In the equation,  $A_1$  is the intercept of the straight lines; and  $B_1$  is the slope of the straight lines. The values of  $A_1$  and  $B_1$  are listed in Table 3.

Therefore, in combination with Equation (6) and parameter values in Table 3, when the confining pressure ranges between 0~25 kPa, the values of  $G_{max}$  of the test samples with void ratios of 1.0 and 0.8 are derived reversely to be 21.908~27.583MPa and 38.518~47.006MPa, respectively.

**Table 3.** Fitting results of  $G_{max}$  and confining pressure  $\sigma$ .

Void ratio $e$	$A_1$	$B_1$
1.0	0.227	21.908
0.8	0.340	38.518

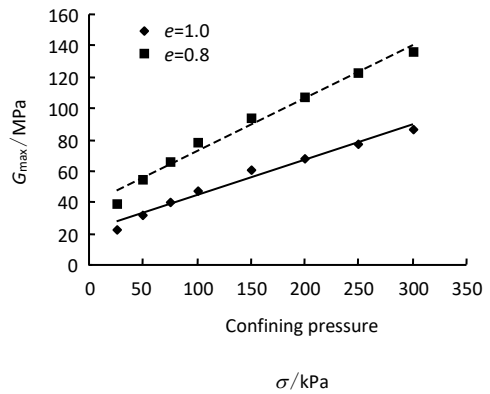


**Fig. 5.** Relationships between  $G_{max}$  and confining pressure  $\sigma$ .

*Varying pattern of  $\lambda_{max}$*

Figure 6 shows the relationship between  $\lambda_{max}$  and confining pressure  $\sigma$  of CAS-1 lunar regolith simulant. Within the range of lower confining pressures (0~25kPa),  $\lambda_{max}$  diminishes rapidly with the increase of  $\sigma$ . Furthermore, it can be seen from the diagram that the two are in a linear relationship and  $\lambda_{max}$  diminishes faster in a linear way when the void ratio  $e$  of the test samples is 1.0; within the range of regular confining pressures (100 ~ 300kPa), the relationship between the maximum equivalent hysteretic viscoelastic damping ratio  $\lambda_{max}$  and  $\sigma$  of CAS-1 lunar regolith simulant undergoes obvious transitions. That is,  $\lambda_{max}$  shows a pattern of slow decrease with the increase of  $\sigma$ . Describe the pattern of how  $\lambda_{max}$  at these two stages varies with  $\sigma$  in a linear relationship, and the uniform expression is:

$$\lambda_{max} = A_2 + B_2\sigma \quad (7)$$

The values of  $A_2$  and  $B_2$  under low and regular confining pressures are listed in Table 4. In combination with Equation (7) and parameter values in Table 4, when the confining pressure

ranges between 0~25 kPa, the values of  $\lambda_{max}$  of the test samples with void ratio of 1.0 and 0.8 are derived reversely to be  $11.240 \times 10^{-2} \sim 9.415 \times 10^{-2}$  and  $6.530 \times 10^{-2} \sim 5.520 \times 10^{-2}$ , respectively.

**Table 4.** Fitting results of  $\lambda_{max}$  and confining pressure  $\sigma$ .

Void ratio $e$	Low confining pressure (25~100 kPa)		Regular confining pressure (100~300 kPa)	
	$A_2$	$B_2$	$A_2$	$B_2$
1.0	-0.073	11.240	-0.008	4.749
0.8	-0.040	6.530	-0.006	3.197

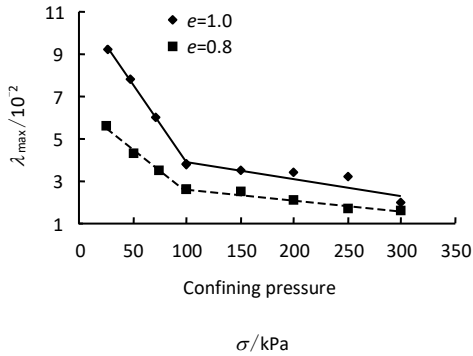


**Fig. 6.** Relationships between  $\lambda_{max}$  and confining pressure  $\sigma$ .

*Varying pattern of the reference shear strain  $\gamma_r$*

Figure 7 shows that the reference shear strain  $\gamma_r$  (fitting parameter) is in good linear relationship with the confining pressure  $\sigma$  and increases with the increase of confining pressure  $\sigma$ . The uniform expression is as follows:

$$\gamma_r = A_3 + B_3\sigma \quad (8)$$

The values of  $A_3$  and  $B_3$  are listed in Table 5.

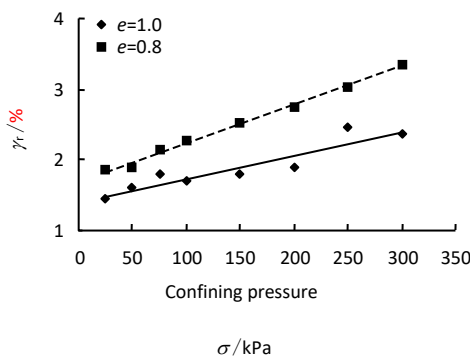


**Fig. 7.** Relationships between  $\gamma_r$  and confining pressure  $\sigma$ .

**Table 5.** Fitting results of  $\gamma_r$  and confining pressure  $\sigma$ .

Void ratio $e$	$A_3$	$B_3$
1.0	0.003	1.407
0.8	0.006	1.685

When the confining pressure ranges between 0~25 kPa, the values of  $\gamma_r$  of the test samples with void ratio of 1.0 and 0.8 are derived reversely to be 1.407% ~ 1.489% and 1.685% ~ 1.822%, respectively.

*Recommended values of  $G/G_{max}$  and  $\lambda$  of lunar regolith simulant*

In the process of sampling, with the gradual increase of the depth of lunar soil layer, the surrounding stress levels will be higher and higher. In this sense, the range values of confining pressure, to some extent reflect the sampling depth of lunar soil. In combination with the test results and fitting curves, in Table 6 relevant test results of test samples with void ratio being 1.0 and 0.8 respectively are listed as recommended values. Such test results are within the range of strain and are obtained from the change of confining pressure. This is of certain reference value for lunar soil sampling.

**Table 6.** Recommended values of  $G/G_{max}$ ,  $\lambda$  and  $\gamma$  of the lunar regolith simulant (0-100 kPa).

Shear strain $\gamma$ / %	$e=1.0$		$e=0.8$	
	$G/G_{max}$	$\lambda/10^{-2}$	$G/G_{max}$	$\lambda/10^{-2}$
0.001	1.000	0.710	1.000	0.570
0.003	0.917	1.220	0.954	1.100
0.005	0.818	2.310	0.886	1.770
0.007	0.758	2.770	0.829	2.200
0.01	0.679	3.400	0.727	3.140
0.02	0.547	4.750	0.617	4.000
0.04	0.369	6.680	0.508	6.130

CONCLUSIONS

(1) By conducting a comparative study of CAS-1 lunar regolith simulant and real lunar soil it was found out that the particle morphology and composition of CAS-1 lunar regolith simulant fall into the category of the particles of real lunar soil and is applicable to dynamic experimental research; by carrying out GDS resonant column experiments, the law by which different void ratios and confining pressures influence the dynamic shear modulus  $G$  and damping ratio  $\gamma$  is found out.

(2) The stress level and the compactness exert a significant effect on the dynamic  $G$  and  $\lambda$ . Under the conditions of real lunar surface, lower stress levels and larger void ratio, there will be smaller  $G$  and larger  $\lambda$ , and with the increase of shear strain, the dynamic shear modulus decreases rapidly whereas the damping ratio increases sharply. This property significantly affects the coring rate of lunar regolith and the completeness of the sample.

(3) By analyzing the test data using the Hardin-Drnevich Hyperbolic Model, the paper works out, for CAS-1 lunar regolith simulant with void ratios of 1.0 and 0.8 respectively, the average fitting curves between  $G/G_{\max}$  and  $\lambda/\lambda_{\max}$  with the change of  $\gamma$  under low and regular confining pressures, and relevant dynamic parameters.

(4) The paper quantitatively analyzes the correlative equation between the maximum dynamic shear modulus  $G_{\max}$ , maximum damping ratio  $\lambda_{\max}$ , reference shear strain  $\gamma_r$  and the confining pressure  $\sigma$  when the void ratio is 1.0 and 0.8, respectively, and accordingly, the values of  $G_{\max}$ ,  $\lambda_{\max}$  and  $\gamma_r$  when the lunar regolith sampling depth ranges between 3~5m and the stress level is between 0 ~ 25kPa. To be specific,  $G_{\max}$  is 21.908 ~ 27.583MPa and 38.518 ~ 47.006MPa, respectively;  $\lambda_{\max}$  is  $11.240 \times 10^{-2} \sim 9.415 \times 10^{-2}$  and  $6.530 \times 10^{-2} \sim 5.520 \times 10^{-2}$ , respectively; and  $\gamma_r$  is 1.407% ~ 1.489% and 1.685% ~ 1.822%, respectively.

The reference values of the dynamic parameters related to CAS-1 lunar regolith simulant given in the above research are of great reference for the ground model test and numerical simulation research in the process of lunar soil sampling.

#### REFERENCES

- 1.H. Kirkici, M.F. Rose, T. Chaloupka, *IEEE Transactions on Dielectrics and Electrical Insulation*, **3**(1), 119 (1996).
- 2.Y.C. Zheng, S.J. Wang, J.M. Feng, *Acta Mineralogica Sinica*, **27**(3/4), 571 (2007).
- 3.S.D. McKay, L.J. Carter, W.W. Woless, *Engineering, Construction, and Operations in Space IV*, New York, 857 (1994).
- 4.B.M. Willmann, W.W. Boles, S. McKay, *Aerospace Engineering*, **8**(2), 77 (1994).
- 5.J.L. Klosky, S. Sture, H.Y. Ko, *Proceedings of the Fifth International Conference on Space 96 Albuquerque*, New York, 680 (1996).
- 6.S.W. Perkins, C.R. Madson, *Journal of Aerospace Engineering*, **9**(1), 1 (1996).
- 7.J.Q. Li, M. Zou, Y. Jia, *Rock and Soil Mechanics*, **29**(6), 1557(2008).
- 8.M. Zou, J.Q. Li, G.M. Liu, *Rock and Soil Mechanics*, **32**(4), 1057 (2011).
- 9.M.J. Jiang, L.Q. Li, F. Liu, *Rock and Soil Mechanics*, **32**(7), 1924 (2011).
10. M.J. Jiang, Y.S. Dai, H. Zhang, *Rock and Soil Mechanics*, **34**(6), 1529 (2013).
11. A. Haydar, S. Stein, B. Susan, *Materials Science and Engineering*, **478**(1), 201 (2008).
12. J.G. Robert, A.G. Marty, A.F. Raymond, *American Institute of Aeronautics and Astronautics*, San Jose:[s. n.], (2006).
13. L.D. Bai, *Chinese Journal of Rock Mechanics and Engineering*, **30**(11), 2366 (2011).
14. L.D. Bai, *Berlin: School of Planning Building Environment*, Technical University of Berlin, 2011.
15. Y.C. Zheng, Z.Y. Ouyang, S.J. Wang, *Journal of Mineralogy and Petrology*, **24**(4), 14 (2004).
16. S.M. Wu, *Soil dynamics*, China Architecture and Building Press, 2000.
17. B.O. Hardin, V.P. Drnevich, *Journal of the Soil Mechanics and Foundations Division, ASCE*, **98**(6), 603 (1972).
18. X.M. Yuan, R. Sun, J. Sun, *Earthquake Engineering and Engineering Vibration*, **20**(4), 133 (2000).
19. H.T. Cai, Y.M. Li, B.S. Ou, *Rock and Soil Mechanics*, **31**(2), 361(2010)